Eur. Phys. J. A **22**, 253–260 (2004)
DOI 10.1140/epja/i2003-10233-9

THE EUROPEAN PHYSICAL JOURNAL A

Decay properties of isomeric states in radium isotopes close to N = 126

F.P. Heßberger[1,a], S. Hofmann[1], I. Kojouharov[1], and D. Ackermann[1,2]

[1] Gesellschaft für Schwerionenforschung mbH, D-64220 Darmstadt, Germany
[2] Institut für Physik, Johannes Gutenberg - Universität Mainz, D-55099 Mainz, Germany

Received: 28 October 2003 / Revised version: 4 April 2004 /
Published online: 9 November 2004 –
Communicated by D. Guerreau

Abstract. Isomeric states in $^{210-215}$Ra have been populated by the decay of the compound nuclei ^{216,220}Ra produced in irradiations of ^{204,208}Pb with ^{12}C at $E_{\rm lab} = (68–136)$ MeV. Published values for γ-ray energies and half-lives were confirmed for $^{212m-215m}$Ra. Our data for ^{210m}Ra agree with the γ-energies and the half-life measured at the RITU separator, University of Jyväskylä (Finland). Its decay pattern is complex. Two series of γ-rays of $E_\gamma = 96.7, 774.6, 578.0, 604.5$ keV and $E_\gamma = 96.7, 602.1, 750.5, 604.5$ keV were observed. A half-life of (2.36 ± 0.04) μs was measured. The isomeric state is attributed to an 8^+ state at $E^* = 2053.8$ keV. A previously unknown isomeric state was assigned to ^{211m}Ra. It has a half-life of (4.0 ± 0.5) μs and it decays by emission of γ-rays with energies of 396.1 keV and 802.0 keV. It is attributed to a $13/2^+$ state at $E^* = 1198.1$ keV.

PACS. 23.60.+e α decay – 27.90.+b $220 \leq A$

1 Introduction

Nuclear structure studies in the vicinity of closed proton and neutron shells are of great interest. Due to a relatively low number of valence protons or neutrons they provide a convenient system for testing the nuclear shell model. In the region below the $N = 126$ shell and $Z > 82$ a vast quantity of data is available up to radon ($Z = 86$) from radioactive-decay studies or in-beam spectroscopy [1]. For heavier nuclei information is rather scarce. Most data are from study of α-decay, which in most cases populates only low-lying levels notably. Only in few cases information on levels in daughter nuclei above 500 keV has been obtained (see refs. [2–4] and references therein). In-beam studies have been performed for ^{211,212,213}Fr [5], ^{212}Ra [6], ^{213}Ra [7], ^{216}Th [8] and ^{206,208,210}Ra [9], which is still the most common method to study decay of highly excited states in nuclei produced in complete fusion reactions. In the trans-lead region production cross-sections for evaporation residues decrease rapidly with increasing proton and/or decreasing neutron numbers and prompt fission becomes the by far most prominent reaction channel. In-beam experiments therefore suffer from high background due to fission products, which completely cover γ-rays emitted from highly excited compound nuclei after particle emission. This problem has been overcome during the last decade by introducing the technique of recoil-decay tagging (RDT) [10]. In RDT γ-rays or conversion electrons detected at the target are correlated with an evaporation residue after separation from the primary beam and fission fragments by a recoil separator and identified by its radioactive decay or by an A and Z measurement in the focal plane. However, this method is restricted to excited states which decay while the recoiling residue is still in view of the γ-ray or electron detectors surrounding the target. Isomeric states with lifetimes comparable to, or longer than the time-of-flight of the recoil through the separator (typically 1–5 μs) may not decay notably before being implanted in the focal plane detection system. Measuring delayed coincidences between the arrival of an evaporation residue in the focal plane and a succeeding γ-decay may thus be regarded as an extension of the RDT for the investigation of isomeric states with lifetimes up to several microseconds. The upper limit will be determined by chance coincidences with background radiation or γ-events from the radioactive decay of the nuclei stopped in the focal plane. In the trans-lead region at or below $N = 126$ this technique has been applied successfully at the RITU separator at the University of Jyväskylä (Finland) for the investigation of ^{216}Th [8] and ^{208m,210m}Ra [9], but for the latter detailed results had not been published so far. To demonstrate the feasability of this technique, we also measured delayed coincidences between evaporation residues and γ-rays in our experiments aimed to study

[a] e-mail: f.p.hessberger@gsi.de

Table 1. List of transitions used for $\alpha - \gamma$-coincidence efficiency estimations.

Isotope	E_α/keV	E_γ/keV	$\epsilon_{\alpha\text{-}\gamma}$ (Run1)	$\epsilon_{\alpha\text{-}\gamma}$ (Run2)	$\epsilon_{\alpha\text{-}\gamma}$ (Run3)	Ref.
^{211}Po	6891	569.7	0.038 ± 0.004	0.065 ± 0.005	0.024 ± 0.002	[4], this work
	6568	897.8	0.023 ± 0.003	0.055 ± 0.006	0.016 ± 0.002	[4], this work
^{213}Ra	6624	110.1	0.06 ± 0.01			[4], this work
^{214}Ra	6505	641.9	0.036 ± 0.004			[4], this work
^{215}Ra	8172	540			0.027 ± 0.001	this work
	6505	836			0.015 ± 0.001	this work
^{216}Ac	8721	853.5	0.034 ± 0.006	0.060 ± 0.004		[4], this work
	8188	937.9	0.025 ± 0.006	0.061 ± 0.003	0.018 ± 0.003	[4], this work
^{217}Th	8725	546.5		0.075 ± 0.007		[3], this work
	8455	822.1		0.073 ± 0.007		[3], this work
^{217m}Pa	9697	466.5		0.088 ± 0.021		[3], this work
	9552, 9553	613.0, 634.31		0.070 ± 0.006		[3], this work
^{247}Md	8421	209.8		0.14 ± 0.02		[16], this work
^{251}Md	7530	295.1		0.12 ± 0.03		[16], this work

fine structure in the α-decay of $^{209-212}$Ra [4]. Besides the isomeric states $^{212m-215m}$Ra already known from data tables [1], we succeeded to identify isomeric states in ^{211m}Ra and ^{210m}Ra. For the latter, our half-life and γ-energies agree with those of the RITU experiment [9].

During the review process of this paper results of a study of isomeric states in ^{209m,210m}Ra were published by Ressler *et al.* [11]. The data presented for ^{210m}Ra are in agreement with our results.

2 Experiment

The experiments were performed at GSI, Darmstadt, using a ^{12}C beam delivered by the high charge state injector with ECR-ion source of the UNILAC accelerator. Beam intensities and energies were $(0.6\text{–}1.2) \times 10^{12}$ ions/s ($\approx$ 100–200 pnA) and (68–136) MeV, respectively. The targets of ^{204}Pb (isotopic enrichment 99.73%), ^{208}Pb (98.69%) with thicknesses of $\approx 450\,\mu$g/cm^2 were evaporated on carbon layers of $40\,\mu$g/cm^2 (upstream) and covered with $5\,\mu$g/cm^2 carbon (downstream). They were mounted on a wheel which rotated synchronously to the beam macro structure [12] (5.4 ms wide pulses at 50 Hz repetition frequency).

The evaporation residues recoiling from the targets with energies of $\approx$ 5 MeV were separated from the primary beam by the velocity filter SHIP [13]. In the focal plane of SHIP they were implanted into a position-sensitive 16-strip PIPS detector ("passivated ion-implanted position-sensitive silicon detector") with an active area of (80×35) mm^2 ("stop detector") [14], used to measure the kinetic energies of the residues as well as subsequent α-decays. Gamma-rays emitted in prompt or delayed coincidence with α-decays or evaporation residues were measured using different types of germanium detectors. Altogether three experimental runs were performed. In Run 1 a High-Purity Ge-Detector (75 mm Ø, 71 mm length) was used. The beam energy was varied in the range (68–136) MeV to measure excitation functions ^{204}Pb$(^{12}$C$, xn)^{216-x}$Ra to identify the isomeric states. In this run we also measured α-decay fine structure of $^{209-212}$Ra. These results are reported in ref. [4] where additional details on the experimental procedure are given. In Run 2 a clover detector consisting of four Ge crystals (70 mm Ø, 140 mm length) which were shaped and assembled to form a block of $(124 \times 124 \times 140)$ mm^3 was used to measure γ-γ–coincidences to prove the correlation of the γ-lines and to clarify the decay patterns. In this run the beam energy was 103 MeV: a compromise between the almost equal production cross-sections for ^{211}Ra and ^{210}Ra expected in the reactions ^{204}Pb$(^{12}$C$, xn)^{216-x}$Ra ($x = 5, 6$) according to HIVAP calculations [15]. In Run 3 half-lives of ^{215m,212m,211m,210m}Ra were estimated by measuring the time intervals between implantation of the evaporation residue and the γ-decay using a time-to-amplitude converter (TAC). The time range was set to 15 μs. The half-life of ^{213m}Ra was obtained from the intensity decrease of the corresponding γ-lines within the 14.6 ms pause between consecutive UNILAC beam bursts. The isotopes were produced either by ^{208}Pb$(^{12}$C$, xn)^{220-x}$Ra ($x = 5, 6, 7$) or by ^{204}Pb$(^{12}$C$, xn)^{216-x}$Ra ($x = 4, 5, 6$). Gamma-rays were registered by a HP-Ge Detector (75 mm Ø, 71 mm length). Since the coincidence time of the data acquisition, triggered by the signal from the implantation of the residue, was only 5 μs and the minimum time distance between two consecutive events registered by the data acquisition was $\approx 15\,\mu$s, the TAC signal as well as the γ-energy signal were delayed by 15 μs.

Alpha-calibration was performed using the literature values of known isotopes which were also produced in the reactions and implanted into the detector as described in [4]. Gamma-calibration was performed with standard energies from ^{152}Eu and ^{133}Ba sources. The overall accuracy of this procedure was ± 5 keV for α- and ± 0.5 keV for γ-energies. The standard intensities of the γ-lines from ^{152}Eu decay were used to estimate the relative efficiency of the Ge detectors. Absolute α-γ (or ER-γ) efficiencies ($p(\alpha\text{-}\gamma)$) were obtained from selected α-transitions accompanied by γ-ray emission of various isotopes, produced either directly in a fusion-evaporation reaction or within

Table 2. Summary of γ-energies and half-lives of $^{210m-215m}$Ra. The intensity values for the 602.1 keV and 604.5 keV lines of ^{210m}Ra refer to the sum of both lines. Therefore they are given in brackets.

^{210m}Ra			^{211m}Ra			^{212m}Ra		
E_γ/keV	i_{rel}	$T_{1/2}/\mu$s	E_γ/keV	i_{rel}	$T_{1/2}/\mu$s	E_γ/keV	i_{rel}	$T_{1/2}/\mu$s
96.7 ± 0.5	0.091 ± 0.007	-	396.1 ± 0.6	0.483 ± 0.004	3.8 ± 0.3	440.2 ± 0.6	0.961 ± 0.013	8.3 ± 0.3
578.0 ± 0.4	1	2.24 ± 0.05	802.0 ± 0.6	1	4.3 ± 0.6	628.6 ± 0.6	0.988 ± 0.015	8.6 ± 0.6
602.1 ± 0.6	(2.146 ± 0.055)	2.44 ± 0.03				824.3 ± 0.6	1	8.0 ± 0.7
604.5 ± 0.6	(2.146 ± 0.055)	2.44 ± 0.03						
750.5 ± 0.4	0.529 ± 0.019	2.42 ± 0.08						
774.6 ± 0.4	0.953 ± 0.029	2.27 ± 0.06						

^{213m}Ra		^{214m}Ra		^{215m}Ra	
E_γ/keV	$T_{1/2}$/ms	E_γ/keV	$T_{1/2}/\mu$s	E_γ/keV	$T_{1/2}/\mu$s
160.4 ± 0.5	2.1 ± 0.1	180.7 ± 0.4	> 15	196.1 ± 0.4	7.6 ± 0.2
545.4 ± 0.5	2.2 ± 0.1	256.8 ± 0.4	> 15	772.3 ± 0.4	7.3 ± 0.3
1061.2 ± 0.5	2.1 ± 0.1	1381.9 ± 0.5	> 15	851.8 ± 0.1	7.5 ± 0.3
				1048.3 ± 0.4	9.0 ± 0.5

the radioactive decay chains of evaporation residues. They were used to scale the relative efficiencies. The experimental efficiencies were calculated using the relation $p(\alpha\text{-}\gamma) = \Sigma(n_{\alpha\gamma})/\Sigma(n_\alpha)$, where $\Sigma(n_{\alpha\gamma})$, $\Sigma(n_\alpha)$ denote the numbers of $(\alpha\text{-}\gamma)$-coincidences and of α-decays. The complete list of isotopes and γ-energies used is presented in table 1. To estimate the efficiency of the clover detector (Run 2) also results from other experiments [3,16] using the same geometry were included. Contrary to [3] the efficiency value here includes the enhancement due to adding coincident signals from different clover segments.

3 Experimental results

3.1 Isomeric states in ^{215,214,213,212}Ra

3.1.1 ^{215}Ra ($T_{1/2} = 7.6\,\mu$s)

An isomeric state at 1878 keV having a half-life of $(7.2 \pm 0.2)\,\mu$s [18] had been previously identified in ^{215}Ra. A tentative spin and parity assignment is $25/2^+$ [17–19]. It is reported to decay either via the transitions $25/2^+$ (56 keV) $\rightarrow$ $21/2^+$ (1048.3 keV, $E3$, 0.18) $\rightarrow$ $15/2^-$ (773.2 keV, $E3$, 1) $\rightarrow$ $9/2^+$ (g.s.) or via $25/2^+$ (56 keV) $\rightarrow$ $21/2^+$ (195.9 keV, $E2$, 0.42) $\rightarrow$ $17/2^+$ (852.4 keV, $E1$, 0.64) $\rightarrow$ $15/2^-$ (773.2 keV, $E3$, 1) $\rightarrow$ $9/2^+$ (g.s.). The data in brackets denote the energies, multipolarities and relative intensities of the γ-transitions. Spin and parity assignments are tentative.

In our irradiation of ^{208}Pb we observed four γ-transitions with half-lives between 7.4 and 9.0 μs and energies fitting within the error bars to the reported values for the decay of ^{215m}Ra. A γ-line of 56 keV, representing the $25/2^+ \rightarrow 21/2^+$ transition, was not observed. Our data are listed in table 2. Our half-life of $(7.6 \pm 0.2)\,\mu$s is comparable with the value of Fukuchi *et al.* [18], but slightly higher than the result of Stuchberry *et al.* of $(6.9 \pm 0.3)\,\mu$s [20].

3.1.2 ^{214m}Ra ($T_{1/2} = 67\,\mu$s)

In the even-even nucleus ^{214}Ra an 8^+ isomeric state at 1865.2 keV having a half-life of $(67 \pm 3)\,\mu$s had been identified previously [21]. It is reported to decay via the transitions 8^+ (45.5 keV) $\rightarrow$ 6^+ (180.4 keV) $\rightarrow$ 4^+ (256.9 keV) $\rightarrow$ 2^+ (1382.4 keV) $\rightarrow$ 0^+ (g.s.). Spin and parity assignments are tentative.

In our irradiation of ^{208}Pb we observed three γ-transitions with energies fitting to the values reported for the decay of ^{214m}Ra within the error bars. Assuming that the relative differences in the intensities of the γ-lines are mainly effected by internal conversion, our experimental values are in best agreement with $E2$ transitions, thus supporting the suggested decay scheme. Half-lives could not be determined. We did not observe a statistically significant decrease of the line intensities within the preset TAC range. Therefore the half-life must be considerably larger than 15 μs. Our data are listed in table 2.

3.1.3 ^{213m}Ra ($T_{1/2} = 2.1$ ms)

The identification of an isomeric state in ^{213}Ra has been reported by Raich *et al.* [7]. The isomeric level was located at $E^* \approx 1770$ keV. A tentative spin and parity assignment $17/2^-$ was given. This was preferred over the $13/2^+$ assignment usually responsible for isomeric states in even-Z odd-N nuclei above $Z = 82$ at $N < 126$ on the basis of the observed α-decay rate. The isomeric state was reported to decay via the transitions $((17/2^-, (13/2^+))$ $(< 10$ keV) $\rightarrow$ $(13/2^-, 11/2^-)$ (160.87 keV) $\rightarrow$ $9/2^-$ (1062.5 keV) $\rightarrow$ $5/2^-$ (546.35 keV) $\rightarrow$ $1/2^-$ (g.s.).

In our experiments we observed three γ-lines with energies fitting the values reported for the decay of ^{213m}Ra. Their half-lives were determined from the decrease of their intensities within the 14.6 ms pause between two consecutive UNILAC beam bursts. An average value of $T_{1/2} = (2.12 \pm 0.02)$ ms was obtained. These data are listed in table 2.

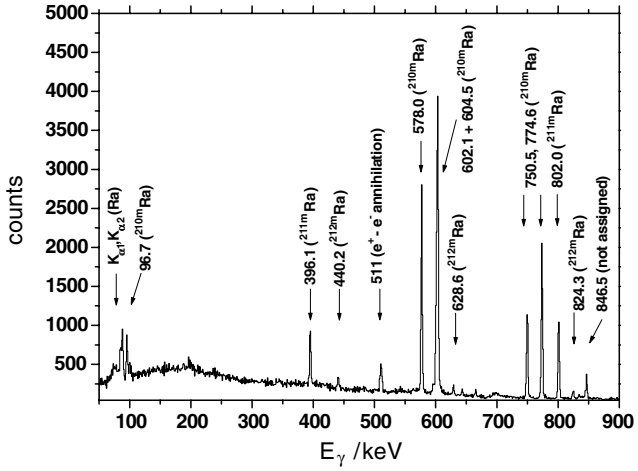

Fig. 1. Gamma-spectra taken in coincidence with evaporation residues in the reaction $^{12}C + ^{204}Pb$ at a bombarding energy $E_{lab} = 103\,MeV$ (Run 2).

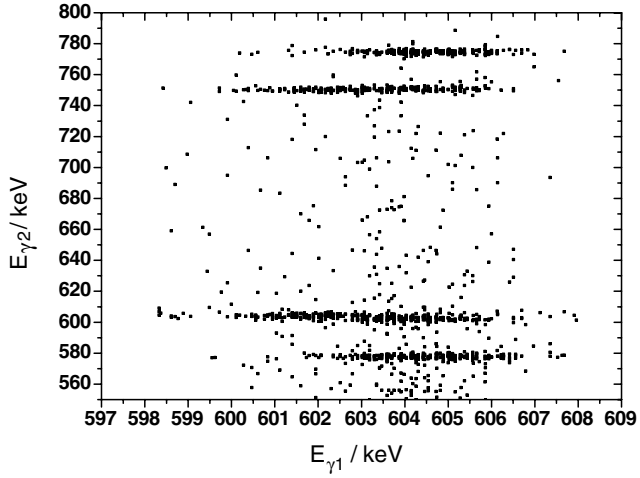

Fig. 2. Two-dimensional plot of γ-γ–coincidences in the energy ranges $E_{\gamma1} = (598–608)\,keV$, $E_{\gamma2} = (550–800)\,keV$.

3.1.4 ^{212m}Ra ($T_{1/2} = 10.5\,\mu s$)

The observation of two isomeric states located at $E^* = 2613.4\,keV$, $T_{1/2} = 0.85\,\mu s$ and at $E^* = 1958.4\,keV$, $T_{1/2} = 10.9\,\mu s$ was reported by Kohno *et al.* [6]. The first was ascribed to an 11^- level, the latter one to an 8^+ level. In our experimental runs using the ^{12}C-beam we only observed γ-lines from the decay of the $10.9\,\mu s$ isomeric state. The $0.85\,\mu s$ isomeric state evidently had already decayed in-flight due to the long flight-time through SHIP of $6.5\,\mu s$. Our measured γ-energies are $440.2 \pm 0.6\,keV$ ($6^+ \rightarrow 4^+$), $824.3 \pm 0.6\,keV$ ($4^+ \rightarrow 2^+$) $628.6 \pm 0.6\,keV$ ($2^+ \rightarrow 0^+$(g.s.)). They agree with the values given by Kohno *et al.* within 1 keV. The transition $8^+ \rightarrow 6^+$ having an energy of 63.3 keV was not observed clearly in our experiment. Indeed we observed in γ-γ–coincidence with the three known lines (18 ± 12) γ-events in the energy interval (60–65) keV, which was twice the average background rate, but due to the large statistical error we do not regard it as a proof. For an $E2$-transition of that energy high conversion coefficients ($\alpha_L \approx 64$, $\alpha_M \approx 18$ [22]) are expected. For the other transitions internal conversion should be of minor importance. For the 440.2 keV transition a value $(\alpha_L + \alpha_M) \approx 0.05$, for the other two transitions values ≤ 0.02 are expected. Indeed we observed within our statistical accuray (± 0.015) equal transition rates for the 628.6 keV and 823.4 keV lines, while for the 440.2 keV line we observed a 3.9% lower intensity.

From these intensity relations we draw the conclusion, that within the given statistical accuracy we observe equal transition rates for γ-rays of the same multipolarity within one decay sequence.

3.2 Identification of ^{211m,210m}Ra

In the irradiation of ^{204}Pb we observed in Run 1 three groups of γ-transitions in delayed coincidence with evaporation residues within $\Delta t = 5\,\mu s$. The lines of each group were characterized by common production characteristics, *i.e.* fixed intensity ratios at different bombarding energies. In Run 2 the affiliation of the lines to each group was further proven by γ-γ–coincidence measurements. As an illustrative example the γ-spectrum taken in coincidence with evaporation residues at $E_{lab} = 103\,MeV$ is shown in fig. 1. Group 1 consisted of three γ-lines of 440.2, 628.6 and 824.3 keV, group 2 of two γ-lines of 396.1 and 802.0 keV, and group 3 of five γ-lines of 96.7, 578.0, 603, 750.5 and 774.6 keV. The γ-line at 603 keV was significantly broader (3.2 keV (FWHM)) compared to the neighbouring line at 578.0 keV (1.8 keV (FWHM)). It was identified in Run 2 an unresolved doublet of 602.1 and 604.5 keV as shown in fig. 2. The γ-lines of group 1 were identical to those attributed to the decay of a $10.5\,\mu s$ isomeric state in ^{212}Ra at $E^* = 1958.4\,keV$ identified by Kohno *et al.* [6] (see sect. 3.1.5).

Excitation functions have been used to assign Groups 2 and 3 to isomeric states in ^{210}Ra and ^{211}Ra. In fig. 3 we have plotted the α-decay rates for $^{209–212}Ra$ (upper panel) and the intensity of a representive γ-ray for each group as a functions of the incident beam energy. The profiles of groups 1 and 2 clearly coincide with that of the α decays of $^{212,211}Ra$, while group 3 coincides with $^{210,209}Ra$. Due to similar α-decay energies the isotopes $^{212,211}Ra$ and $^{210,210}Ra$ cannot be discriminated individually. In fig. 3 it can also be seen that the maximum intensity of the 628.6 keV line occurs at a lower energy than that of the 396.1 keV line. Having assigned of the 628.6 keV transition to the decay of ^{212m}Ra, the 396.1 keV line consequently is attributed to the decay of an isomeric state ^{211m}Ra. This interpretation is also supported by the results of HIVAP [15] calculations which are shown in the lower panel fig. 3. The maxima for the 628.6 keV and for the 396.1 keV lines roughly agree with calculated maxima for ^{212}Ra and ^{211}Ra.

The representative of group 3, the (602.1, 604.5 keV) γ-line has its maximum intensity at higher beam energies. A comparison with the HIVAP calculations clearly

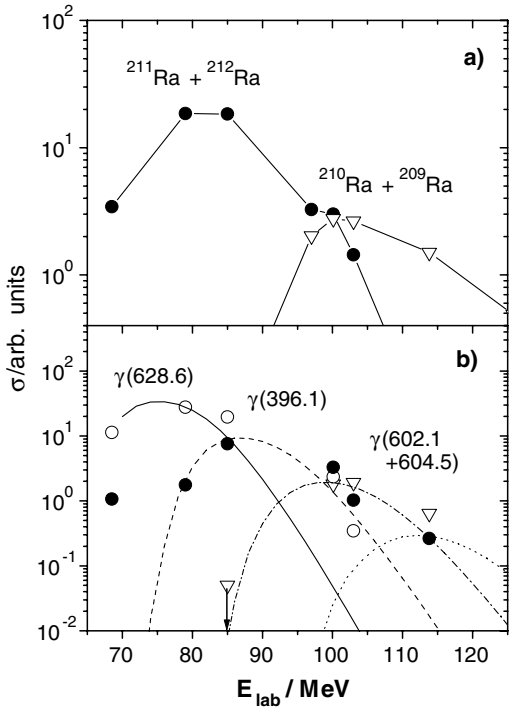

Fig. 3. Excitation functions for $^{209-212}$Ra in the reaction ^{12}C+ ^{204}Pb from (a) α-decays of ^{209,210}Ra (open triangles), ^{211,212}Ra (full circles) or (b) γ-lines. Alpha-lines of ^{211}Ra (6907 keV), ^{212}Ra (6898 keV) or ^{209}Ra (7003 keV), ^{210}Ra (7003 keV) are not resolved (data from [4]); each isomeric state is represented by one γ-line: ^{212m}Ra (628.6 keV, open circles), ^{211m}Ra (396.1 keV, full circles), ^{210m}Ra (602.1, 604.5 keV, open triangles). The lines in b) represent the results of a HIVAP calculation: ^{212}Ra (full line), ^{211}Ra (dashed line), ^{210}Ra (dashed-dotted line), ^{209}Ra (dotted line).

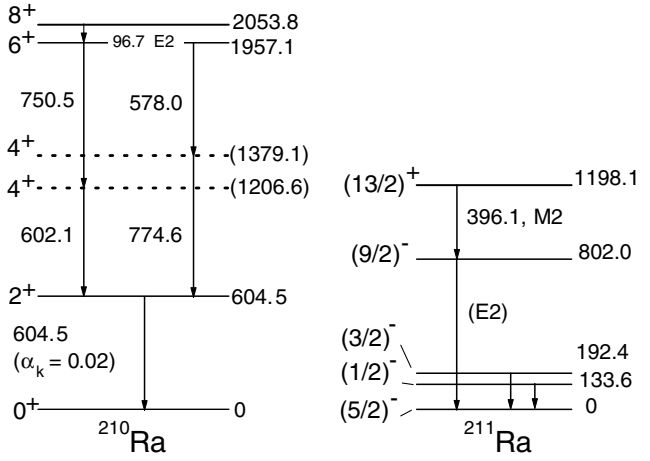

Fig. 4. Suggested decay schemes for ^{210m}Ra and ^{211m}Ra. Energies are given in keV. The energies of the 4^+ levels in ^{210}Ra could not be determined unambiguously from our experiment. Their placement has to be regarded as tentative (see detailed discussion in the text).

shows a better agreement with ^{210}Ra than with ^{209}Ra. This group of transitions is therefore assigned to an isomeric state ^{210m}Ra.

3.3 Decay of ^{211m}Ra and ^{210m}Ra

To investigate the decay properties of the isomeric states in more detail, we performed a second and a third experimental run. The second run was devoted to investigate the decay pattern by measuring γ-γ–coincidences, while in the third the half-lives were measured. As a check for the reliability of our method we used the results obtained for ^{212m,215m}Ra.

3.3.1 Decay of ^{210m}Ra

The decay pattern of ^{210m}Ra is complicated and could be clarified only on the basis of γ-γ–coincidence measurements. As a summary of the analysis of these measurements we state:
a) the lines at 96.7 and 604.5 keV are coincident with all other γ-lines;
b) the lines at 578.0 and 774.6 keV are coincident with each other and with 96.7 and 604.5 keV, but not with 750.5 and 602.1 keV;
c) the lines at 602.1 and 750.5 keV are coincident with each other and with 96.7 and 604.5 keV, but not with 578.0 and 774.6 keV;
d) the sum energies 602.1 keV + 750.5 keV = 1352.6 keV and 578.0 keV + 774.6 keV = 1352.6 keV are equal within the error bars (±0.6 keV).

We thus conclude that the decay of ^{210m}Ra occurs in four steps, but runs through different intermediate states. The four-step decay suggests for the isomeric state an 8^+ level decaying by four $E2$ transitions. To obtain a long-living isomeric state the transition energy $8^+ \rightarrow 6^+$ must be necessarily low. Consequently the line at 96.7 keV is attributed to that transition. Its low intensity compared to the other lines is ascribed to a strong conversion branch of the transition. Based on the line intensities a conversion coefficient of $\alpha_L = 12.5 \pm 3.5$ is obtained which is best in agreement with $\alpha_L + \alpha_M = 11.1$ [22] expected for an $E2$ transition. (K conversion is energetically not possible.) The 604.5 keV line, also observed in coincidence with all other lines is attributed to the $2^+ \rightarrow 0^+$ (g.s.) transition since a) similar 2^+ excitation energies are observed for all neighbouring even-even nuclei with $Z = (84–88)$ and $N < 126$, and b) otherwise two 2^+-levels had to exist in ^{210}Ra at $E^* < 1$ MeV, a feature that is not observed in other even-even nuclei. Thus we assign the other two groups (578.5 + 774.6 and 602.1 + 750.5) to the decay $6^+ \rightarrow 4^+ \rightarrow 2^+$, running via different 4^+ states. Indeed two 4^+ states in the range $E^* = 1.0–1.5$ MeV have been identified in the neighbouring even-even nuclei ^{206,208,210}Rn. The energies of these levels can given only tentatively, leading to the tentative decay scheme shown in fig. 4, which is discussed in more detail in sect. 4. Transitions between the 4^+ states have not been observed. Figure 4 suggests a $4^+ \rightarrow 4^+$ transition energy

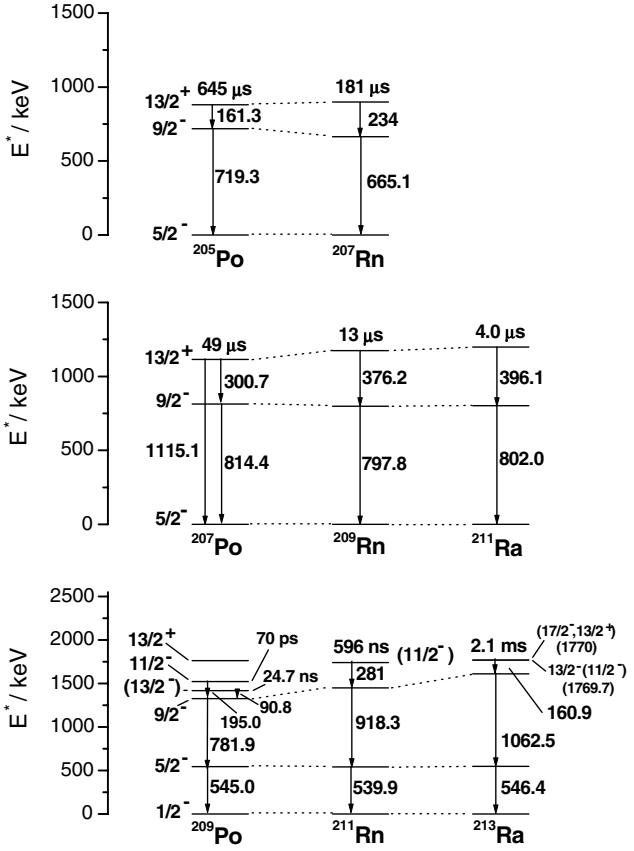

Fig. 5. Comparison of the decay schemes of isomeric states in $N = 121, 123$ and 125 isotopes.

of 172.5 keV ($M1$). However, neither a line at 172.5 keV was observed in the singles spectrum, nor coincidences of 172.5 keV with 96.7, 578.0, 602.1 or 604.5 keV were observed. Respecting $M1$ conversion coefficients $\alpha_K = 2.74$, $\alpha_L = 0.54$ and $\alpha_M = 0.15$ we obtain an intensity limit $i(4^+ \to 4^+)/i(4^+ \to 2^+) < 0.1$.

The half-lives measured for the individual γ-lines are given in table 2. A mean value from all lines of $2.36 \pm 0.05\,\mu$s was obtained.

3.3.2 Decay of ^{211m}Ra

The γ-lines attributed to the decay of the isomeric state in ^{211m}Ra are at 396.1 ± 0.6 and 802.0 ± 0.6 keV. The line at 396.1 keV was found only in coincidence with 802.0 keV, while the line at 802.0 keV was found in coincidence with the 396.1 keV line, and an additional group of lines in the range (80–105) keV that fit to the energies of the $K_{\alpha 1}$, $K_{\alpha 2}$, $K_{\beta 1}$, $K_{\beta' 2}$-X-ray lines of radium. This finding means that the 396.1 keV transition is converted. The intensity ratio between the γ-lines is $i(396.1)/i(802.0) = 0.483$. In analogy to the discussion in 3.3.1 we ascribe the missing intensity to internal conversion and obtain a conversion coefficient $\alpha = 1.07 \pm 0.044$, where $\alpha = \alpha_K + \alpha_L + \alpha_M$. The line intensity of the X-rays can be used to determine the $K/(L+M)$ conversion ratio. We obtain $\alpha_K/\alpha = 0.44 \pm 0.03$. According to [22] the most probable multipolarities are $E4$ ($\alpha = 1.46$, $\alpha_K/\alpha = 0.19$) and $M2$ ($\alpha = 1.06$, $\alpha_K/\alpha = 0.75$). We assign $M2$ to the transition, since a) the conversion coefficients are closer to $M2$ than to $E4$ and b) a Weisskopf estimation results in a half-life of 0.09 μs for the $M2$ transition, but 175 s for an $E4$ transition, which is seven orders of magnitude higher than the experimental value.

The decay scheme is shown in fig. 4. We locate the isomeric state at $E^* = 1198.1$ keV. The decay energies are quite similar to those of the $N = 123$ isotones ^{209}Rn and ^{207}Po as indicated in fig. 5. From these systematics it is thus straightforward to assign the isomeric state to a $13/2^+$ level decaying via a $9/2^-$ level into the $5/2^-$ ground state. This interpretation is supported by the assigned multipolarity $M2$ to the 395 keV transition, which is expected for a $13/2^+ \to 9/2^-$ decay.

It should be remarked that two unassigned γ-lines of 395.6 ± 0.5 keV and 801.2 ± 0.5 keV reported by Ressler *et al.* [11] agree with our data for ^{211m}Ra.

4 Discussion

The existence of isomeric states having half-lives similar to that of the ground state and decaying by emission of α-particles or electron capture is a widespread phenomenom in odd-mass nuclei with even atomic numbers in the region $Z \geq 82$, $N < 118$. Their α-decay energies are typically around 100 keV higher than those of α-particles from the ground state. These isomeric states have been identified, or assigned to an $i_{13/2}$ neutron hole configuration, resulting in spin and parity of $13/2^+$. The energies of these states exhibit similar trends for isotopes of lead, polonium and radon. The excitation energies are typically lower than 300 keV for $N < 113$. Approaching the $N = 126$ shell the energies of these levels increase and hence the isomeric lifetimes decrease steeply. At $N = 123$ half-lives are found to be 5.04 ms (^{205}Pb), 49 μs (^{207}Po), and 13 μs (^{209}Rn). In ^{207}Pb ($N = 125$) the $13/2^+$ state is located at $E^* = 1633.368$ keV, having a half-life of 0.805 s, while in ^{209}Po it was located at 1760.96 keV, but was not identified as an isomeric state.

Since it is known that shell strengths of neutron and proton shells mutually influence each other [23], the sensitive energy dependence of the $13/2^+$ level can be regarded as one probe to indicate the disappearance (or not) of the $N = 126$ shell with increasing proton numbers above the $Z = 82$ proton shell. Information on the location of the $13/2^+$ state in radium isotopes is therefore desirable. Isomeric states decaying by α emission have been identified in ^{207,205,203}Ra [24,25]. They are tentatively assigned to the $13/2^+$ level since they decay into the corresponding levels in the radon daughter nuclei by unhindered transitions. The location of the $13/2^+$ level could, in principle, be obtained from the difference of the Q_α values, provided the ground-state α-decay populates the ground state in the daughter nuclues, which, however, is not evident *a priori*. In data compilations [26] a value of (470±100) keV is given

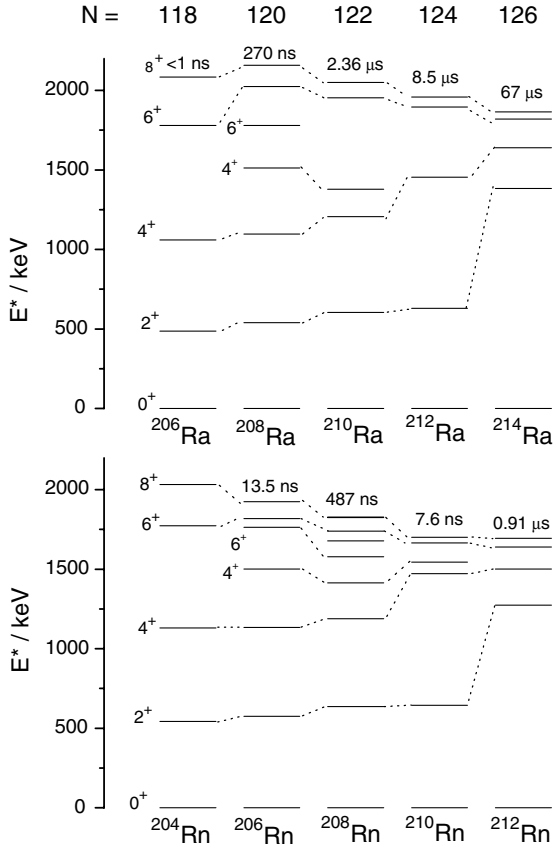

Fig. 6. Comparison of (partial) level schemes of even-even radon and radium nuclei in the range $N = 118$–126. For better presentation, for some nuclei not all levels reported in the literature are shown. The dotted lines are to guide the eye.

for ^{207m}Ra. In ^{213}Ra a 2.1 ms isomeric state has been identified, but is attributed to a $17/2^-$ state. So the result for ^{211m}Ra represents the only reliable data on the location of the $13/2^+$ level in radium isotopes. Compared to the neighbouring ($N = 123$)-isotone ^{209}Rn only a slight shift of ≈ 25 keV in the energy of the $13/2^+$ level is observed, while the shift for $9/2^-$ is even smaller (≈ 4 keV), indicating a similar nuclear structure of both isotopes. This is supported by the energies of low-lying levels populated by α-decay of ^{215}Th and ^{213}Ra, respectively. No γ-lines that could be attributed to the decay of a $13/2^+$ isomeric state in ^{209}Ra were observed in our experiments. As seen in fig. 5, the mean decrease in half-lives in the series ^{207}Po $\rightarrow$ ^{209}Rn $\rightarrow$ ^{211}Ra and ^{205}Po $\rightarrow$ ^{207}Rn is a factor of about 3.5 per step. One could expect a half-life of $\approx 50\,\mu$s for an isomeric state in ^{209}Ra, which is certainly too long to observe a γ-ray intensity sufficient for an unambiguous identification within our $5\,\mu$s coincidence interval.

In even-even nuclei the occurrence of 8^+ isomeric states is widespread, which is caused by a low energy difference between 8^+ and 6^+ states. As seen in fig. 6 both levels are decreasing in energy and moving together for $N > 118$ when approaching the neutron shell at $N = 126$, which leads to an increase of the half-lives. Figure 6 exhibits two other trends: States with low spins (2^+, (lowest) 4^+) increase in energy, which is especially evident in the large energy increase of the lowest 2^+ - state from $N = 124$ to $N = 126$.

In the neighbouring even-even nuclei ^{212}Ra [6] and ^{208}Rn [27] the isomeric state is ascribed to the 8^+ member of the $\pi h_{9/2}^6 \nu = 2$ or the $\pi h_{9/2}^4 \nu = 2$ multiplet, respectively. Shell model calculations performed for ^{208}Rn [27] result also in a multiplet built up on a neutron hole configuration ($\nu f_{5/2}^{-2}$) with 2^+ and 4^+ states at $E^* = 806$ keV and $E^* = 1180$ keV, respectively. While in the case of ^{208}Rn and seemingly for ^{212}Ra the decay of the isomeric state runs nearly exclusively through the 6^+ and 4^+ states of the proton excitation configuration, in the case of ^{210}Ra the 4^+ states of both, the proton and the neutron hole excitation configurations are populated with almost equal intensity. According to the excitation energies of the 4^+ state(s) in ^{208}Rn and ^{212}Ra, we assign one of the low-energy γ-lines (602.1 or 578.0 keV) to the $6^+ \rightarrow 4^+$ (proton excitation) transition and one of the high-energy γ-lines (774.6 or 750.5 keV) to the $6^+ \rightarrow 4^+$ (neutron hole excitation) transition. An unambiguous assignment cannot be given on the basis of our data. Our tentative choice is based on a comparison of the intensity ratio $i(774.6\,\text{keV})/i(750.5\,\text{keV}) = 1.8 \pm 0.2$ with lifetime ratios obtained from Weisskopf estimations, $\tau(602.1, E2)/\tau(774.6, E2) = 3.5$, $\tau(750.5, E2)/\tau(774.6, E2) = 1.2$, and $\tau(750.5, E2)/\tau(578.0, E2) = 0.27$. The ratio $(\tau(\gamma1)/\tau(\gamma2))/(i(\gamma2)/i(\gamma1))$ may then be regarded as a hindrance of the transition $\gamma2$ compared to $\gamma1$. Identifying the 602.1 keV line as $6^+ \rightarrow 4^+$ (proton excitation) transition and the 774.6 keV line as $6^+ \rightarrow 4^+$ (neutron hole excitation) transition, we obtain a hindrance factor of ≈ 1.9 for the 774.6 keV transition, while in the case of identifying the 578.0 keV line as $6^+ \rightarrow 4^+$ (proton excitation) transition and the 750.5 keV line as $6^+ \rightarrow 4^+$ (neutron hole excitation) transition, we obtain a hindrance factor of ≈ 6.6 for the 750.5 keV transition. Since a direct transition $6^+ \rightarrow 4^+$ (neutron hole excitation) was not observed in ^{208}Rn [27] at all, it rather seems justified to assign the more hindered transition in ^{210}Ra to $6^+ \rightarrow 4^+$ (neutron hole excitation).

In cases where data are available, as ^{208}Rn [27], only a low intensity of the $4^+ \rightarrow 4^+$ transition, compared to the $4^+ \rightarrow 2^+$ transition was observed, indicating strong hindrance of the $M1$ transitions between the two different 4^+ configurations, which is in-line with our non-observation of such a transition in ^{210}Ra in our experiment.

5 Summary and outlook

The method of measuring delayed coincidences between γ-rays and evaporation residues, implanted into a Si-detector in the focal plane of SHIP after in-flight separation from the primary beam has been demonstrated to be a powerful technique to investigate isomeric states in the microsecond range. Decay properties of already reported isomers could be verified and a new isomeric state, ^{211m}Ra, was identified. Its decay properties resemble those

of the $N = 123$ isotone ^{209m}Rn rather than those of the next heavier odd-mass radium isotope ^{213m}Ra. This may indicate that the systematic behavior of the $13/2^+$ states known from nuclei with lighter atomic numbers is also preserved for the radium isotopes. In this aspect it seems interesting also to search for a $13/2^+$ isomeric state in ^{209}Ra, which would be the link between the known cases ^{207m}Ra and ^{211m}Ra. With respect to the systematics in the half-lives of the $13/2^+$ states in the $N = 121, 123$ nuclei (fig. 5) one would expect a value $T_{1/2} \approx 50\,\mu$s for ^{209m}Ra. It should be detectable with the technique used above if the time for delayed coincidences is increased. Certainly this will lead to a higher background from random coincidences, but γ-γ–coincidences would act as a purification filter. For higher atomic numbers it would be interesting to extend the search towards thorium isotopes. The cross-sections there are rather small, only up to a few microbarns [28], but at high beam intensities the sensitivity of the method presented is sufficient for successful measurements.

References

1. R.B. Firestone, V.S. Shirley, C.M. Baglin, S.Y. Frank Chu, J. Zipkin, *Table of Isotopes*, 8th edition (John Wiley & Sons, Inc., New York, Chicester, Brisbane, Toronto, Singapore, 1996).
2. F.P. Heßberger, S. Hofmann, D. Ackermann, V. Ninov, M. Leino, S. Saro, A. Andreyev, A. Lavrentev, A.G. Popeko, A.V. Yeremin, Eur. Phys. J. A **8**, 521 (2000).
3. F.P. Heßberger, S. Hofmann, I. Kojouharov, D. Ackermann, S. Antalic, P. Cagarda, B. Kindler, B. Lommel, R. Mann, A.G. Popeko, S. Saro, J. Uusitalo, A.V. Yeremin, Eur. Phys. J. A **15**, 335 (2002).
4. F.P. Heßberger, S. Hofmann, D. Ackermann, Eur. Phys. J. A **16**, 365 (2003).
5. A.P. Byrne, G.D. Dracoulis, C. Fahlander, H. Hübel, A.R. Poletti, A.E. Stuchbery, J. Gerl, R.F. Davie, S.J. Poletti, Nucl. Phys. A **448**, 137 (1986).
6. T. Kohno, M. Adachi, S. Fukuda, M. Taya, M. Fukuda, H. Taketani, Y. Gono, M. Sugawara, Y. Ishikawa, Phys. Rev. C **33**, 392 (1986).
7. D.G. Raich, H.R. Bowman, R.E. Eppley, J.O. Rasmussen, I. Rezanka, Z. Phys. A **279**, 301 (1976).
8. K. Hauschild, M. Rejmund, H. Grawe, E. Caurier, F. Nowacki, F. Becker, Y. Le Coz, W. Korten, J. Döring, M. Gorska, K. Schmidt, O. Dorvaux, K. Helariutta, P. Jones, R. Julin, S. Juutinen, H. Kettunen, M. Leino, M. Muikku, P. Nieminen, P. Rahkila, J. Uusitalo, F. Azaiez, M. Belleguic, Phys. Rev. Lett. **87**, 072501 (2001).
9. J.F.C. Cocks, the JUROSPHERE Collaboration, J. Phys. G: Nucl. Part. Phys. **25**, 839 (1999).
10. K.-H. Schmidt, R.S. Simon, J.-G. Keller, F.P. Heßberger, G. Münzenberg, B. Quint, H.-G. Clerc, W. Schwab, U. Gollerthan, C.-C. Sahm, Phys. Lett. B **168**, 39 (1986).
11. J.J. Ressler, C.W. Beausang, H. Ai, H. Amro, M.A. Caprio, R.F. Casten, A.A. Hecht, S.D. Langdown, E.A. McCutchan, D.A. Meyer, P.H. Regan, M.J.S. Sciacchitano, A. Yamamoto, N.V. Zamfir, Phys. Rev. C **69**, 034331 (2004).
12. H. Folger, W. Hartmann, F.P. Heßberger, S. Hofmann, J. Klemm, G. Münzenberg, V. Ninov, W. Thalheimer, P. Armbruster, Nucl. Instrum. Methods Phys. Res. A **362**, 64 (1995).
13. G. Münzenberg, W. Faust, S. Hofmann, P. Armbruster, K. Güttner, H. Ewald, Nucl. Instrum. Methods **161**, 65 (1979).
14. S. Hofmann, V. Ninov, F.P. Heßberger, P. Armbruster, H. Folger, G. Münzenberg, H.J. Schött, A.G. Popeko, A.V. Yeremin, A.N. Andreyev, S. Saro, R. Janik, M. Leino, Z. Phys. A **350**, 277 (1995).
15. W. Reisdorf, Z. Phys. A **300**, 227 (1981).
16. F.P. Heßberger, S. Hofmann, D. Ackermann, S. Antalic, P. Cagarda, I. Kojouharov, P. Kuusiniemi, R. Mann, S. Saro, GSI Scientific Report 2003, GSI 2004-1, 3 (2004).
17. T. Lönnroth, C. Baktash, Physica Scripta **28**, 459 (1983).
18. Y. Fukuchi, T. Komatsubara, H. Sakamoto, T. Aoki, K. Furuno, J. Phys. Soc. Jpn. **57**, 2976 (1988).
19. G.D. Dracoulis, F. Riess, A.E. Stuchbery, R.A. Bark, S.L. Gupta, A.M. Baxter, M. Kruse, Nucl. Phys. A **493**, 145 (1989).
20. A.E. Stuchbery, G.D. Dracoulis, T. Kibedi, A.P. Byrne, B. Fabricius, A.R. Poletti, G.J. Lane, A.M. Baxter, Nucl. Phys. A **461**, 401 (1998).
21. T.W. Conlon, Nucl. Phys. A **189**, 65 (1972).
22. R.S. Hager, E.C. Seltzer, Nuclear Data A **4**, 1 (1968).
23. K.-H. Schmidt, D. Vermeulen, *Proceedings Atomic Masses and Fundamental Constants 6*, edited by J.A. Nolan jr., W. Benenson (Plenum Press, New York and London, 1980) p. 119.
24. F.P. Heßberger, S. Hofmann, G. Münzenberg, A.B. Quint, K. Sümmerer, P. Armbruster, Europhys. Lett. **3**, 895 (1987).
25. M. Leino, J. Uusitalo, R.G. Allatt, P. Armbruster, T. Enqvist, K. Eskola, S. Hofmann, S. Hurskanen, A. Jokinen, V. Ninov, R.D. Page, W.H. Trzaska, Z. Phys. A **355**, 157 (1996).
26. M.J. Martin, Nucl. Data Sheets **70**, 315 (1993).
27. W.J. Triggs, A.R. Poletti, G.D. Dracoulis, C. Fahlander, A.P. Byrne, Nucl. Phys. A **395**, 274 (1983).
28. D. Vermeulen, H.-G. Clerc, C.-C. Sahm, K.-H. Schmidt, J.G. Keller, G. Münzenberg, W. Reisdorf, Z. Phys. A **318**, 157 (1984).